

# MODELING THE TENSILE BEHAVIOR OF FIBERS WITH GEOMETRICAL AND STRUCTURAL IRREGULARITIES

*W. He and X. Wang*

*School of Engineering and Technology, Deakin University  
Geelong, VIC 3217 Australia, xwang@deakin.edu.au*

(Received: November 19, 2002- Accepted in Revised Form: August 11, 2003)

**Abstract** Virtually all fibers exhibit some dimensional and structural irregularities. These include the conventional textile fibers, the high-performance brittle fibers and even the newly developed nano-fibers. In recent years, we have systematically examined the effect of fiber dimensional irregularities on the mechanical behavior of the irregular fibers. This paper extends our research to include the combined effect of dimensional and structural irregularities, using the finite element method (FEM). The dimensional irregularities are represented by sine waves with a 30 % magnitude of diameter variation while the structural irregularities are represented by longitudinal and horizontal cavities distributed within the fiber structure. The results indicate that fiber geometrical or dimensional variations have a marked influence on the tensile properties of the fiber. It affects not only the values of the breaking load and extension, but also the shape of the load-extension curves. The fiber structural irregularities simulated in this study appear to have little effect on the shape of the load-extension curves.

**Key Words** Fiber, Irregularity, Tensile Behavior, Modeling, Structural Variations

**چکیده** تمام الیافها بطور طبیعی بی نظمی ابعادی و ساختاری از خود نشان می دهند. از آن جمله می توان به الیافهای معمولی نساجی، الیافهای پرکار ترد و حتی الیافهای نو ظهور نانو اشاره کرد. تاثیر بی نظمیهای ابعادی بر رفتار مکانیکی الیاف در سالهای اخیر بطور سیستماتیک توسط تیم تحقیقاتی ما بررسی شده است. این مقاله در راستای توسعه تحقیقات قبلی برای تلفیق تاثیر بی نظمی ابعادی با بی نظمی ساختاری از طریق بکارگیری روش اجزای محدود تحریر شده است. بی نظمیهای ابعادی بوسیله موج سینوسی با دامنه تغییر قطر ۳۰٪ در نظر گرفته شده و بی نظمیهای ساختاری توسط حفرات طولی و افقی توزیع شده در ساختار الیاف نمایش داده شده اند. نتایج نشان می دهد که تغییرات هندسی و ابعادی الیاف تاثیر بسزایی بر خواص کششی الیاف دارد؛ بطوریکه نه تنها بر مقادیر نیرو و تغییر طول شکست تاثیر می گذارد، بلکه بر شکل منحنیهای کشش نیز اثر دارد. این نتایج همچنین نشان می دهد که بی نظمیهای ساختاری شبیه سازی شده در این تحقیق بر دیاگرامهای کششی تنها تاثیر اندکی دارد.

## 1. INTRODUCTION

Most fibers are highly irregular in both dimension and structure, and this is particularly true with textile materials. During fiber processing, various cuts and deformations may be introduced to the fibers by sharp mechanical elements such as carding tooth, hence exacerbating the fiber structural and geometrical irregularities. The effect of fiber irregularities on fiber tensile properties has long been recognized. Considerable research work on wool fibers has been conducted on how fiber

tensile behavior depends on fiber diameter (or cross-sectional area) variation and structural irregularity. Among them, many works (Banky and Slen [1,2], Kenny and Chaikin [3], Collins and Chaikin [4], Shah and Whiteley [5], Wang [6], Zhang and Wang [7], Zhang [8]) are focused on fiber dimensional variation and its effect on the tensile behavior of fibers. Some works (Collins [9] and Collins and Chaikin [10-15]) are concerned with both dimensional variation and structural irregularity of fibers. These works have indicated that fiber irregularities would change the shape of

**TABLE 1. Parameters for FE Model in Tensile Analysis.**

Properties	Value
Young's modulus (MPa)	1700*
Poisson's ratio	0.35
True stress at break (MPa)	258.5*
Specimen diameter ( $\mu\text{m}$ )	20
Specimen length (mm)	0.1

\* Obtained from a pen-grown Corriedale wool (Collins [9]).

stress-strain curves and would reduce the fiber breaking stress and strain with increasing fiber variations. The effect of structural variability within wool fibers on the fiber tensile behavior has mainly been examined with a number of models based on the "two-phase" structure, as proposed by Feughelman [16,17]. A few papers (Mason [18], Andrews [19], Makinson [20]) have been published on the effect of the structural variability on the tensile behavior of wool fibers, in which the notched and modulated wool fibers are examined. The results showed that fibers notched to a shallow depth had substantially the same strength properties as a normal fiber and the strength reduction was small for modulated fibers.

Recently, more attention has been paid to the wool fiber breakage or damage due to the interaction of fibers and metallic elements during fiber processing. Different types of fiber damage may be induced during processing, such as transverse and longitudinal cracks, cavities, and crushed regions, etc. (Gharehaghaji and Johnson [21,22], Gharehaghaji [23]). Even the ancient technique of opening wool and cotton fibers with vibrating strings can cause different forms of structural damage (Wang [24]), which all lead to fiber weakening and affect the mechanical properties of fibers.

Wang and Wang [25,26] investigated fiber strength loss at processing stages, too. The study shows that it can cause different degrees of reduction in strength in each processing stage due to the different conditions of fiber/fiber and

fiber/metallic elements interactions.

There has been considerable interest in brittle materials such as glass, carbon, and ceramics fibers, etc. for high-strength and high-modulus composite applications. The mechanical properties, especially tensile strength, of these fibers can significantly influence the fracture behavior of the composites. The structure of these fibers is usually imperfect. For instance, surface cracks, internal flaws and different distributions of flaws often exist in the fibers (Dalmaz et al. [27] and Zinck et al. [28]).

Many works are, therefore, focused on the effect of fiber structural variation on its strength. An analysis of the relationship between strength and structure of ceramic fibers was provided by Sawye et al. [29], who demonstrated that fiber tensile strength was controlled by critical flaws and pointed out that process improvements and elimination of large defects could result in increased tensile strength.

Taylor et al. [30] examined the effects of flaw location, flaw size and flaw type on the strength of ceramic-grade Nicalon fiber. They suggested that flaw size played a more prominent role than flaw type in determining fiber strength values. Jones et al. [31] examined the effects of flaw location on the strength of carbon filaments and found that fibers with internal flaws were generally stronger than fibers with the same flaws at the edge of the fiber surface.

Further research is needed to clarify this situation. In addition, investigation using simulation and mathematical modeling also showed that the cracks and flaws affect fiber strength (Karbhari and Wilkins [32], Knoff [33]). Numerical models using finite element methods have also been used to analyze related problems in brittle fibers and other composite materials (Wisnom [34], Tong et al. [35], Firmature and Rahman [36], Zhang and Subhash [37]). However, these papers only worked on structural irregularity of fiber, without considering diameter variation along the fiber length.

In this paper, we use the non-linear finite element analysis to model the structural and dimensional variations of fibers, and analyze the tensile behavior of these fibers.

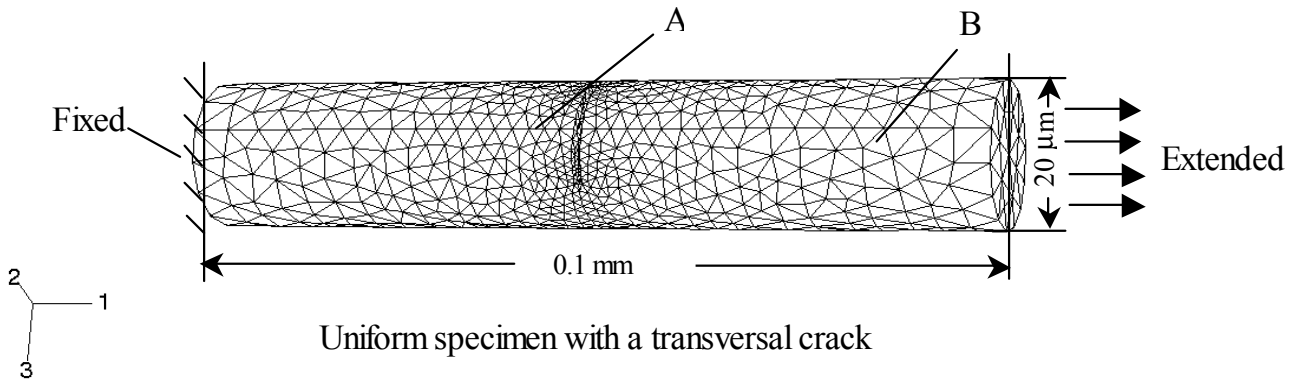


Figure 1. Specimen geometry mesh, dimension and loading conditions.

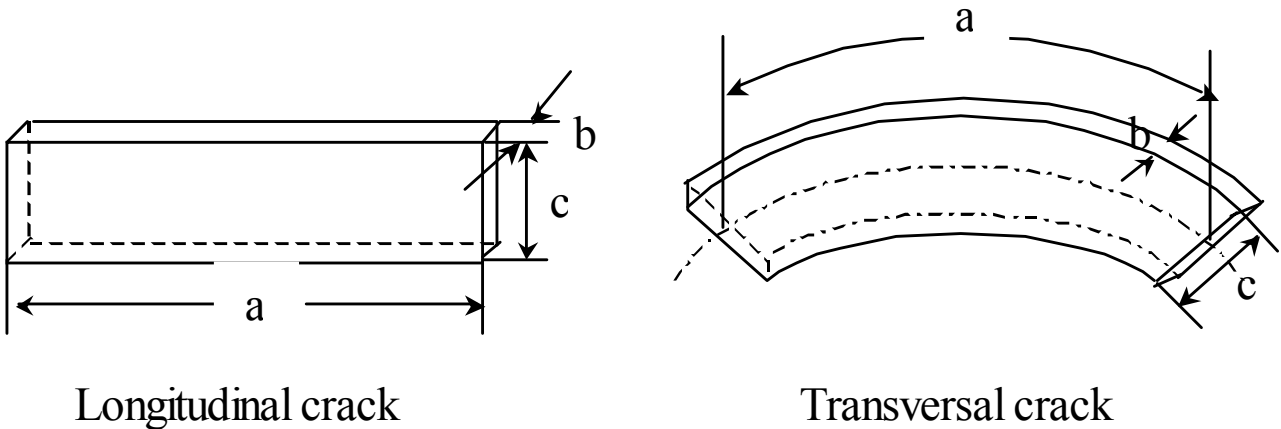


Figure 2. Geometry and dimension of crack.

## 2. FINITE-ELEMENT MODEL

**2.1 Fiber Assumption** In this study, the cross-section of fiber specimen is assumed to be circular along the fiber length, so that fiber diameter variation can represent its dimensional irregularity. Structural variability of fiber and the combined structural and dimensional irregularities of fiber are considered, respectively. For the former, we assume that the different types of flaw (e.g., longitudinal crack, transverse crack and round cavities) are located in a uniform fiber (constant fiber diameter). For the latter, these defects are distributed in a fiber with 30% level of diameter variation, which follows the sine wave

pattern. In order to investigate the effect of fiber non-uniformity on fiber tensile behavior, we need to know the tensile behavior of the fiber without any structural and dimensional irregularities. Therefore, a tensile behavior similar to that of uniform pen-grown Corriedale wool (Collins [9]) is chosen and the nominal stress-strain curve of this kind of wool fiber is used. In addition, we assume that the length and average diameter of the simulated fiber specimen are 0.1 mm and 20 μm, respectively, in all cases simulated in this study. Relevant details concerning the fiber specimens used for the simulations are listed in Table 1.

**2.2 Model Description** ABAQUS/CAE (version

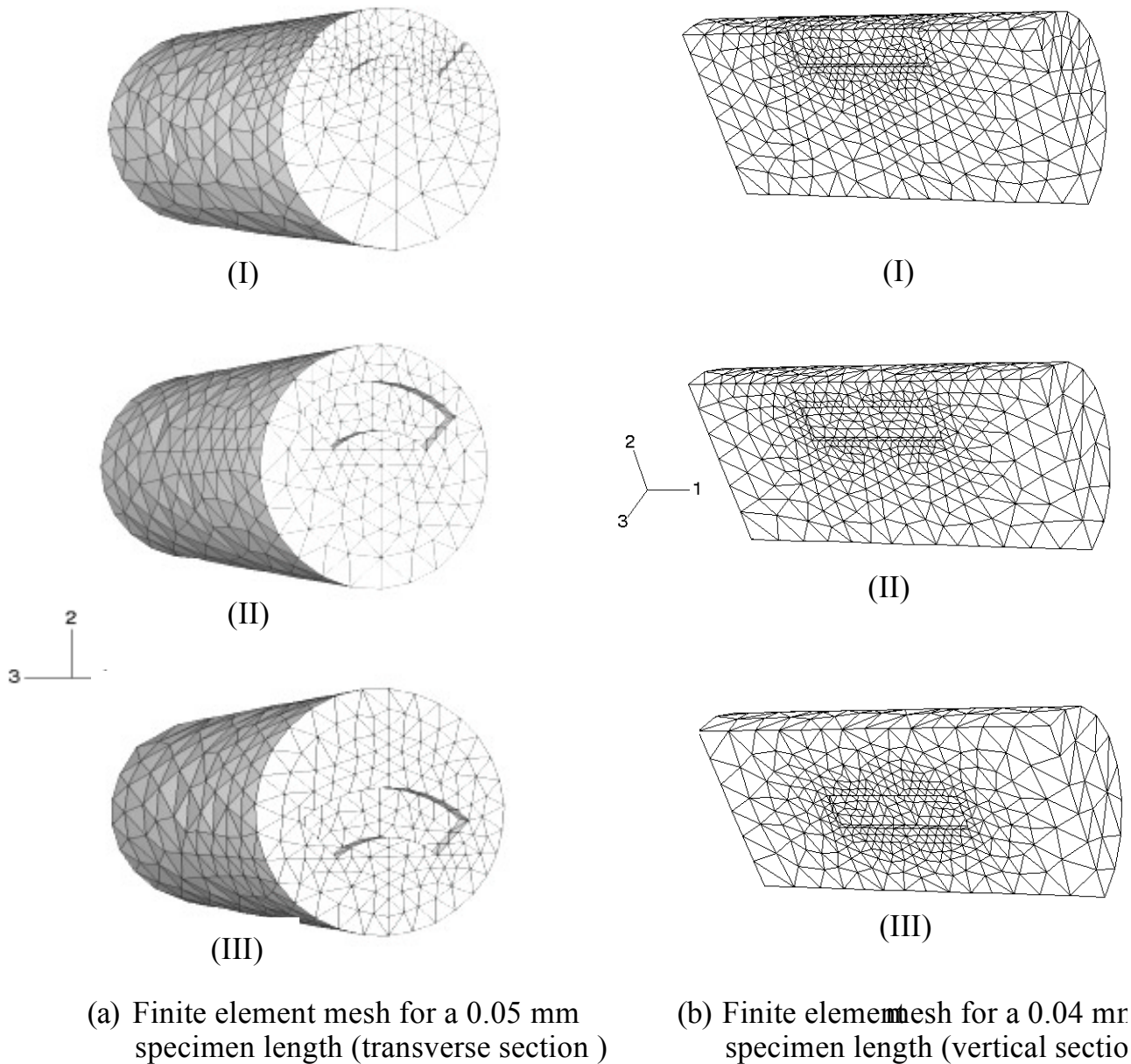


**Figure 3.** Graphical representation of the simulated specimens with (a) transverse crack and (b) longitudinal crack.

6.1) [38] is used in this study to create three-dimensional finite element models for the simulation. Physical and material properties are assigned to the simulated fiber, together with load and boundary conditions. Complex geometries can be difficult to mesh with hexahedral (brick-shaped) elements;

therefore, the element type of C3D4 is chosen for this particular application. In addition, a large number of elements (fine meshes) have been used for the different simulated cases to ensure simulation accuracy. To reduce computational time, an irregular mesh is applied to the model. A finer mesh is

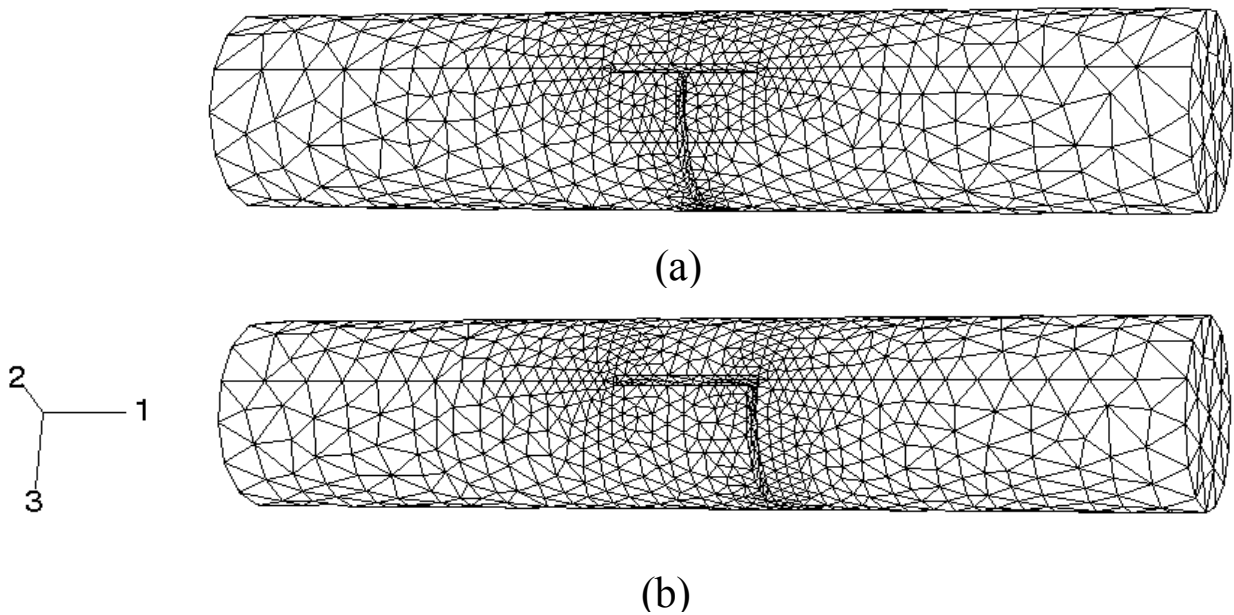


Figure 4. Finite element model: mesh of the fiber specimen with (a) T-crack and (b) L-crack.

chosen near the crack or cavity region where the stress concentration exists and accurate results are needed (see Figure 1A), and a relatively coarser mesh at distances farther away (see Figure 1B). The total number of elements is controlled at 8500-9500/0.1 mm, and the average distortion of elements is 1.64-1.68, and the worst distortion is less than 3 for minimizing the mesh distortion. In the analysis, one end (left) of the fiber specimen is constrained and the other end (right) is extended along the fiber axial direction until the fiber is broken. Figure 1 gives a fiber specimen geometry mesh, dimension and loading conditions used in the analysis.

### 3. RESULTS AND DISCUSSION

**3.1 Effect of Fiber Structural Irregularity on Fiber Tensile Behavior** In this part of study, dimensional variation is neglected, the fiber specimen is regarded as a uniform column and the diameter is 20  $\mu\text{m}$ .

**3.1.1 Effect of Crack Type, Location and Size on Fiber Tensile Behavior** Two types of

cracks, transverse and longitudinal cracks, are investigated here and the size of the crack is illustrated in Figure 2. Different cases are simulated. Case 1 represents a uniform fiber specimen. Case 2 (Figure 3a) and Case 3 (Figure 3b) simulate the fiber specimen with transverse and longitudinal cracks, respectively, and these cracks also occur at different positions in the fiber specimen (Figure 3, I, II and III). Case 4 simulates the fiber specimen with longitudinal surface crack, but the size of the crack is different (see Table 2, Case 4). Further, case 5 simulates a fiber with two types of combined transverse and longitudinal cracks on the fiber surface, as shown in Figure 4.

Simulation results for the different cases are listed in Table 2. For all cases (except case 1), the crack weakens the fiber specimen, as expected. Results for case 2 and case 3 indicate that the transverse crack led to more reduction in breaking load and breaking extension than the longitudinal crack. When the fiber specimen with a transverse crack is stretched, the tensile stress concentrates on the crack and grows rapidly with increasing fiber elongation, as illustrated in Figure 5. The maximum tensile stress of 258.5 MPa (true stress at break, as given in Table 1) is reached at an

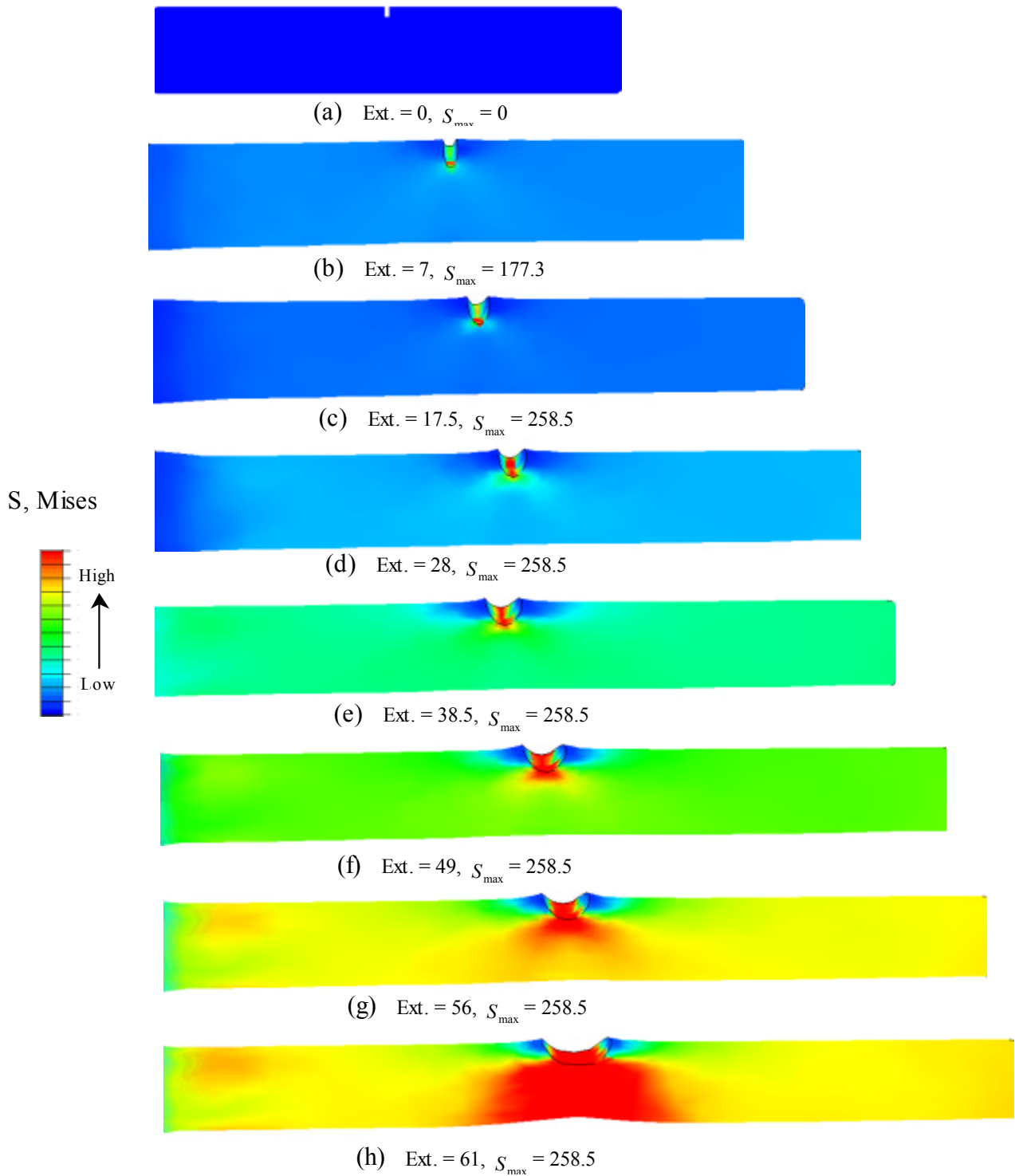


**Figure 5.** The contours of equivalent stress of uniform fiber with a transverse crack during successive extensions.

extension of 17.5 % (see Figure 5c).

During subsequent stretching, the transverse

crack becomes wider and propagates towards the inside across the fiber specimen (see Figure 5c to

**TABLE 2. Simulation Conditions and Data for Fiber Specimen with Different Cracks.**

Simulation cases		Crack type	Crack size (a x b x c) ( $\mu\text{m}$ )	Simulation results	
				Breaking load (g)	Breaking extension (%)
Case 1		No crack	-	4.96	65.6
Case 2	I	Transverse crack	15 x 1 x 4	4.53	61.1
	II			4.64	61.8
	III			4.66	62.0
Case 3	I	Longitudinal crack		4.94	64.8
	II			4.92	64.7
	III			4.88	64.4
Case 4	I	Longitudinal crack	15 x 1 x 8	4.80	63.5
	II		15 x 2 x 4	4.84	64.2
Case 5	T-crack	Combined crack	15 x 1 x 4	4.38	59.2
	L-crack			4.49	60.4

h), leading to the failure of the fiber specimen. However, for the fiber with a longitudinal crack, the tensile stress still concentrates on the crack, but it develops slowly with fiber extension (see Figure 6). The breaking stress (258.5 MPa) is reached at a much higher extension of 59.9 % (see Figure 6 e). This is because the cross-sectional area of the fiber with a longitudinal crack is much larger than that with a transverse crack of similar size. So the breaking load and breaking extension of the fiber with the transverse crack is lower than that with the longitudinal crack. Despite of the fact that stress development and stress distribution pattern is different for the fiber specimen with the transverse crack or longitudinal crack, the fiber fracture for both cases always occurs at the crack region.

It is interesting to note that in case 2 I, II, III and case 3 I, II, III, as the cracks are at different locations (along the radius as shown in Figure 3), the breaking load and breaking extension of the fiber vary slightly. While the tensile properties

are not very sensitive to the crack location, the trend for longitudinal and transverse cracks is the opposite. With the transverse cracks (case 2), surface crack is more serious than interior crack, which is consistent with results obtained by Jones et al. [31]. For longitudinal cracks, the reverse trend is observed (case 3, Table 2), namely, the lower breaking load of fiber accompanies the crack located closer to the fiber center, which is also in agreement with the experimental results obtained by Taylor et al. [30]. These simulation results therefore indicate that the effect of fiber structural flaw (defect) on the fiber tensile behavior depends on the geometrical shape and distribution of the flaw or crack. Nevertheless, the effect of longitudinal cracks on fiber tensile properties is very small. The interior longitudinal crack is similar to medullae in animal fibers. Experimental results obtained from modulated wool fibers by Mason [18] and Andrews [19] have indicated that the effect of medullae on the tensile behavior of wool is small,

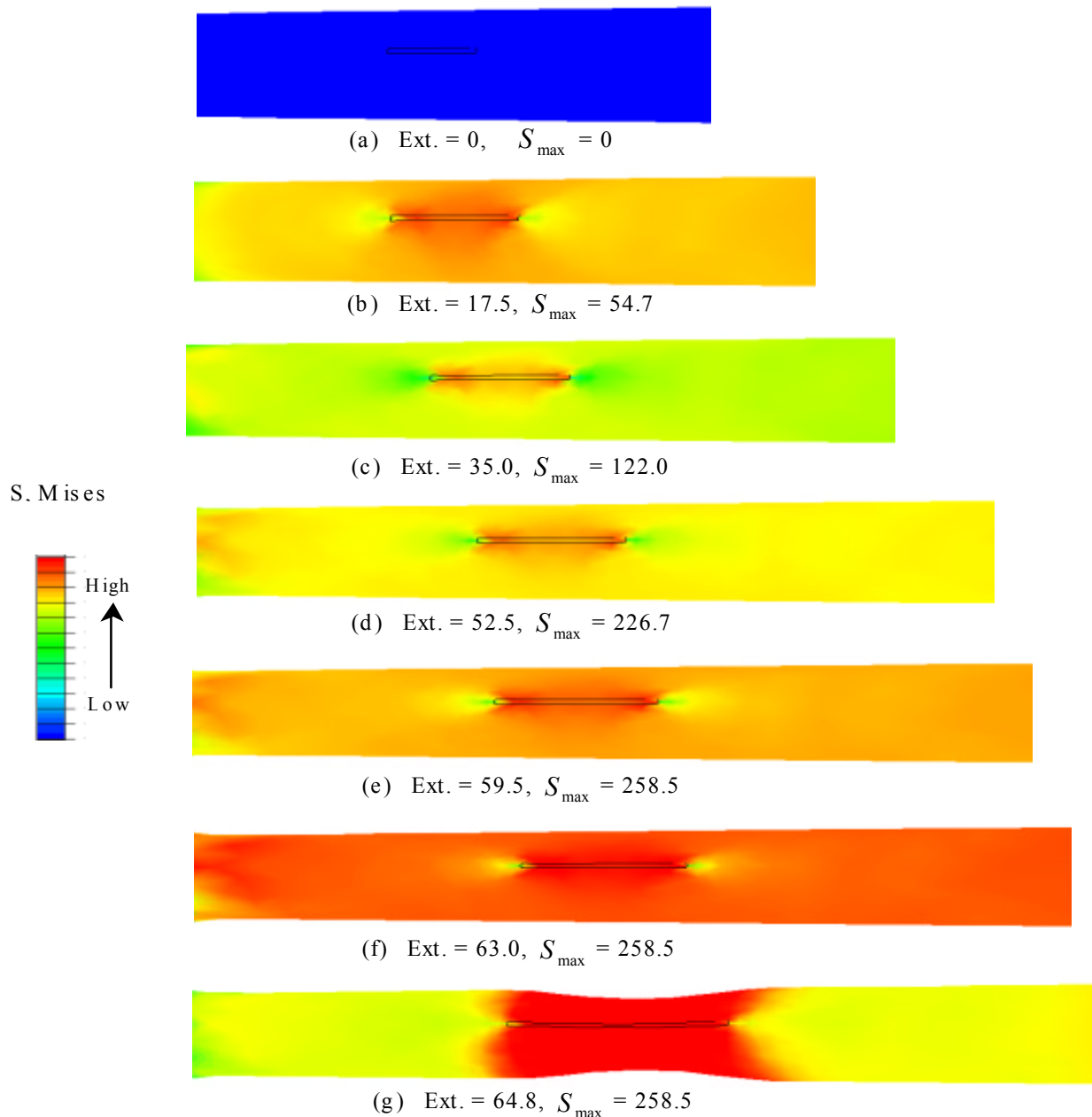


**Figure 6.** The contours of equivalent stress of uniform fiber with a longitudinal crack during successive extensions.

which supports the simulation results here.

In addition, increasing the depth (case 4 I) or width (case 4 II) of the crack will result in a reduction of the breaking load and breaking extension (see Table 2, case 4) as the weak region of fiber increases. Especially, for fiber with a deep crack, the minimum fiber diameter decreases and the fiber is weaker than the fiber with a wide but

shallow crack. This is consistent with the weakest-link theory.

For case 5, the fiber has a combination of transverse and longitudinal cracks (T-crack and L-crack) (see Figure 4), and its breaking load and breaking extension drop more than the fiber with only a transverse crack or a longitudinal crack. Meanwhile, for the fiber with a T-crack, it might



**TABLE 3. Simulation Conditions and Data for Fiber Specimen with Different Distribution and Size of Interior Cavities.**

Simulation cases		Radius of cavity (R) ( $\mu\text{m}$ )	Simulation results	
			Breaking load (g)	Breaking extension (%)
Case 1	I	3	4.80	64.4
	II		4.75	64.0
	III		4.78	63.7
	IV		4.72	63.4
	V		4.51	60.4
Case 2	I	2	4.90	64.8
	II	4	4.49	62.3

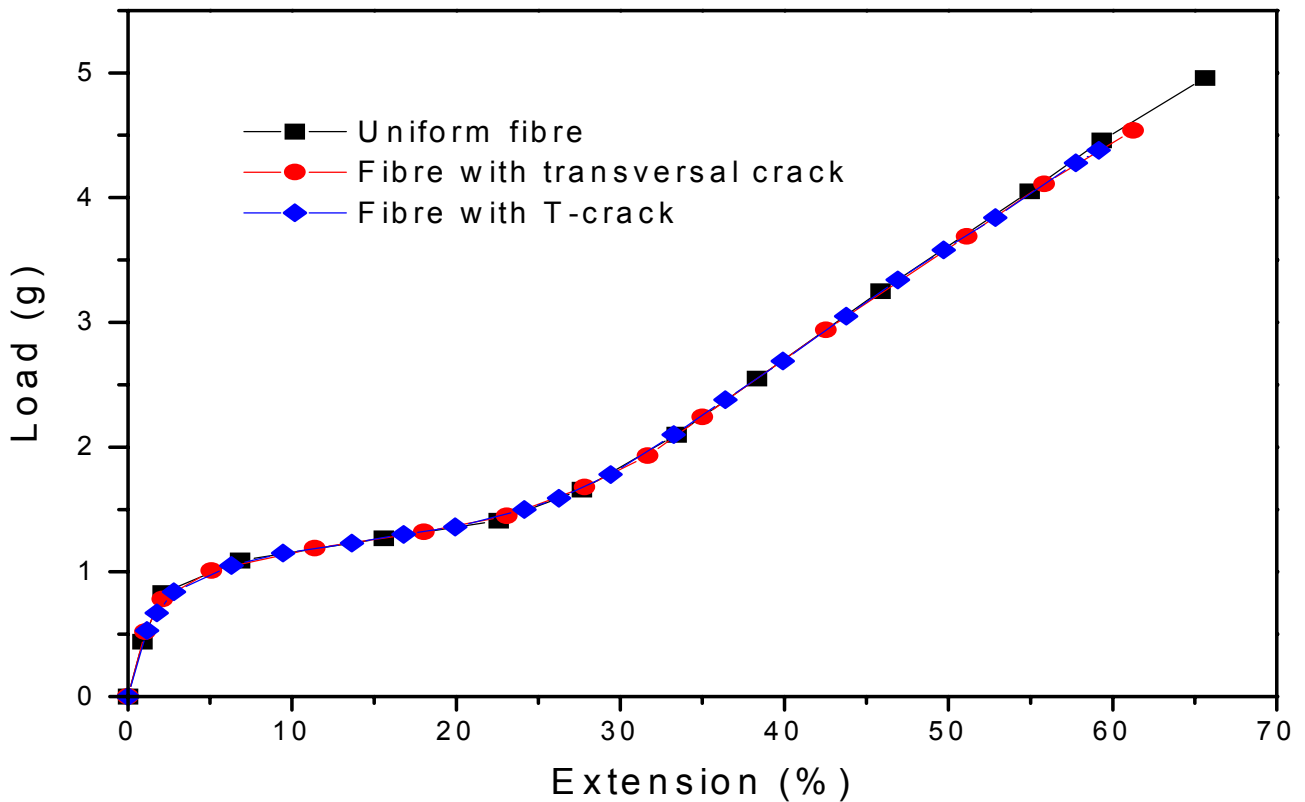


**Figure 7.** Load-extension curves for a uniform fiber and fibers with different cracks.

be easier to be stretched and deformed in the joint. Therefore, the values of breaking load and breaking extension of the fiber are lower than the fiber with

a L-crack.

It is worth mentioning that for the different cases simulated, the shapes of the load-extension

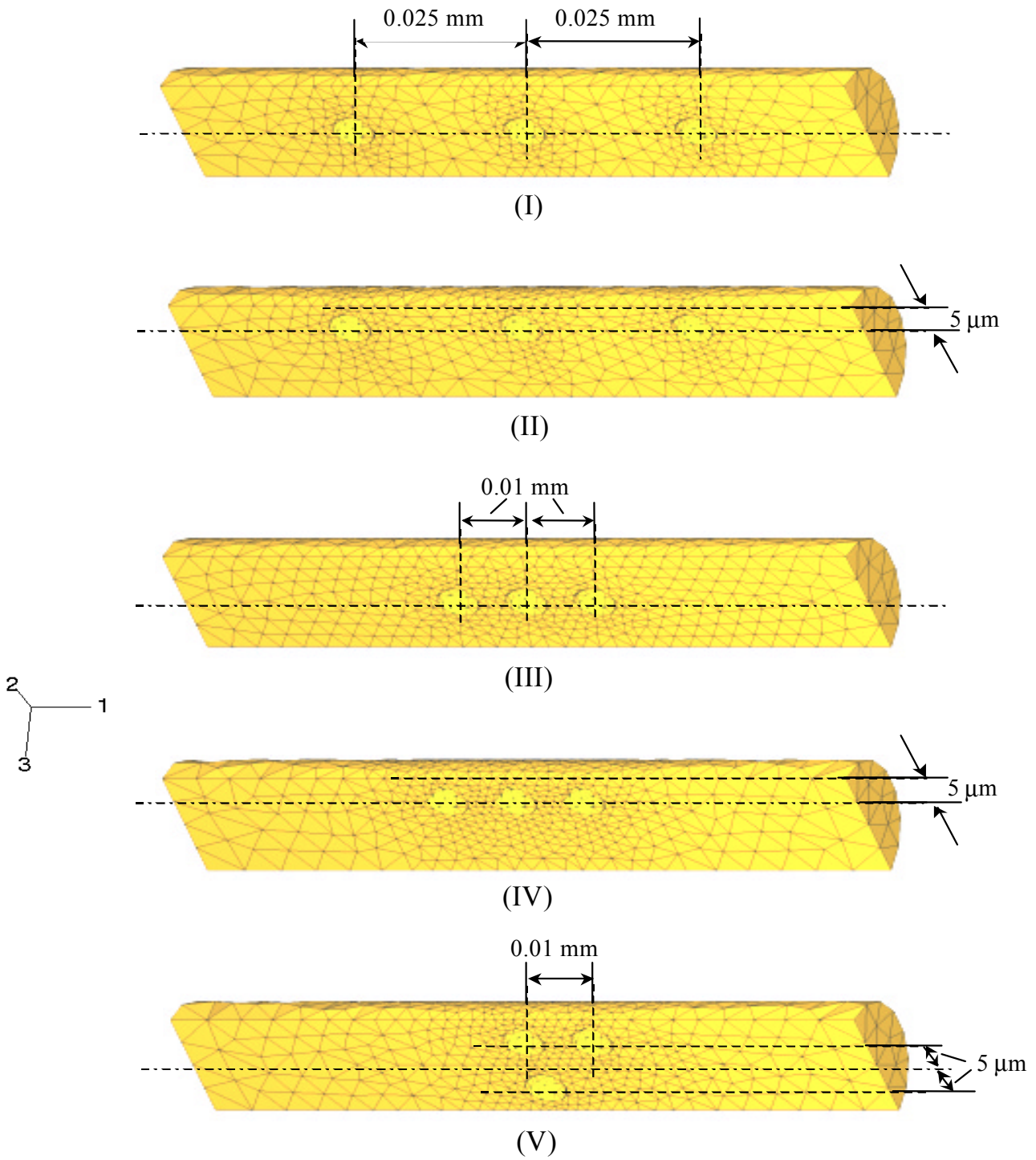


**Figure 8.** Finite element mesh of different distribution of interior cavities.

curve of fiber specimen are all the same. The load-extension curves also overlap. Only the values at

the breaking point vary with the crack type, location and size. Figure 7 gives the load-extension

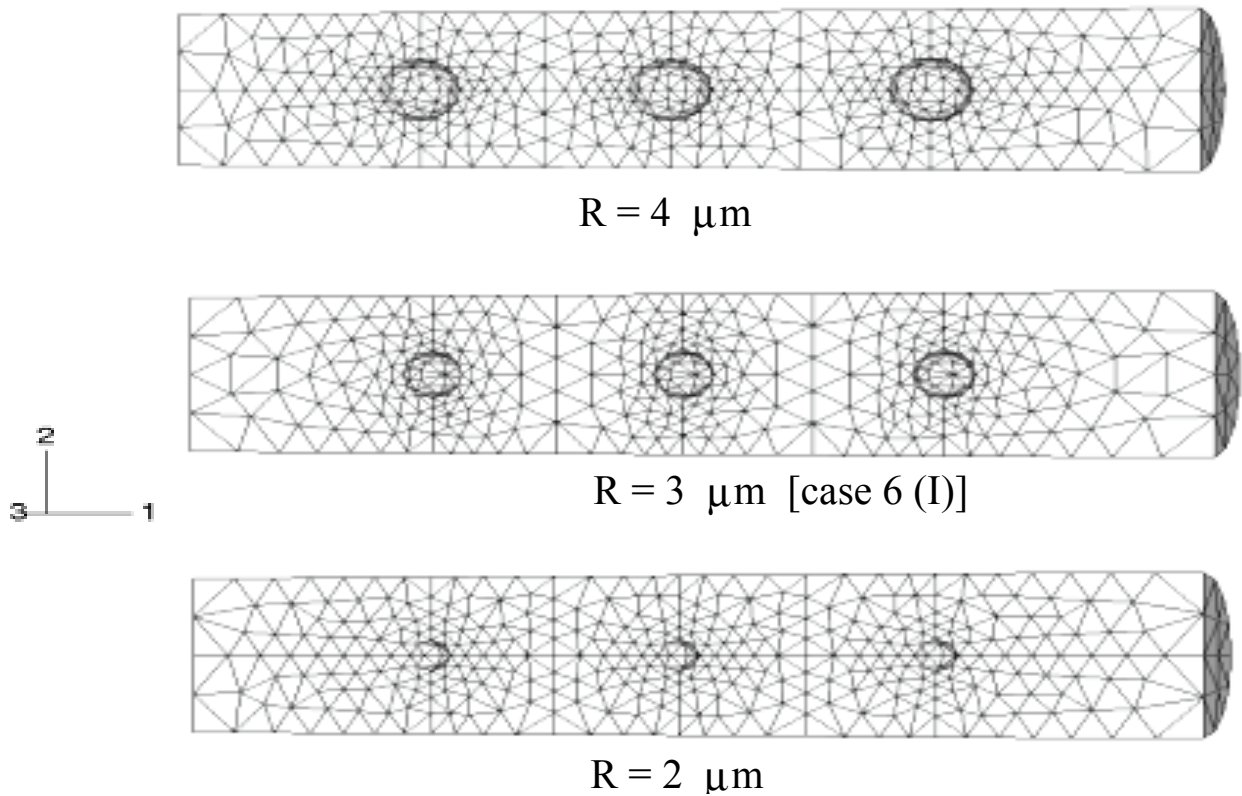


Figure 9. Finite element mesh of different sizes of interior cavities.

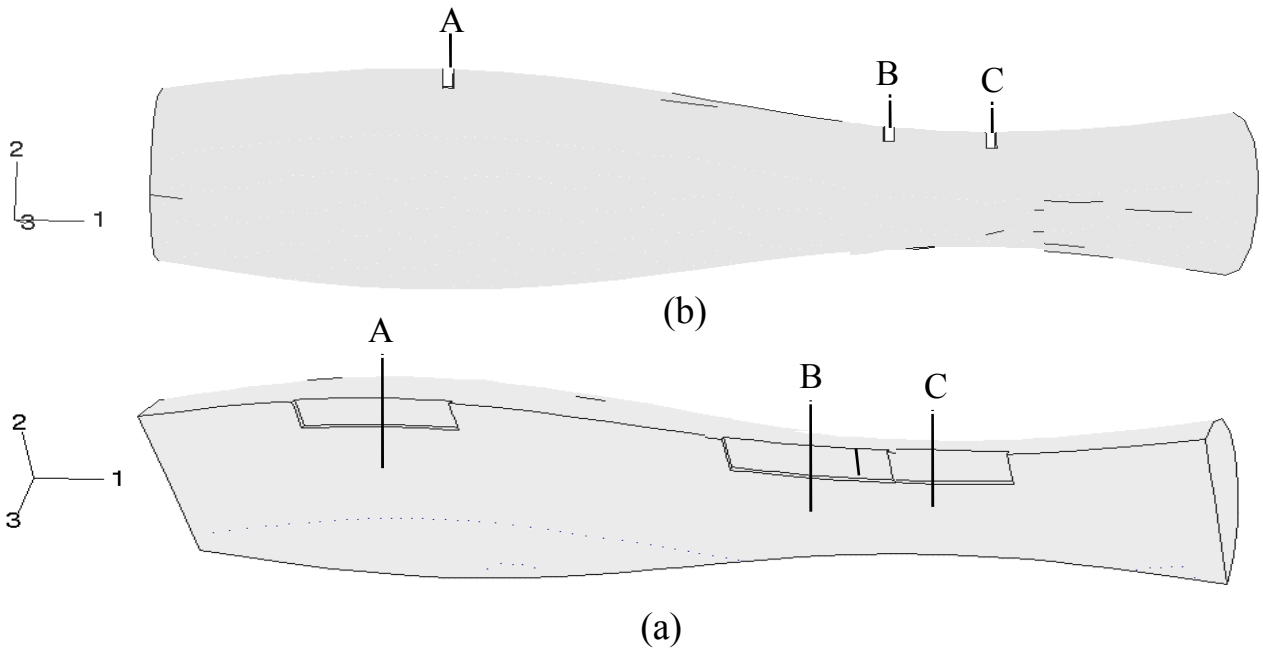
curves of uniform fiber and fiber with the transverse cracks and T-crack.

### 3.1.2 Effect of Distribution and Size of Interior Cavities on Fiber Tensile Behavior

As indicated in Table 3, we simulated two cases here. Case 1 represents fiber specimen with three interior cavities and these cavities all have the same radius ( $R = 3 \mu\text{m}$ ), but their distribution in the specimen is different. Three cavities in case 1 I to case 1 IV are arranged along the fiber specimen length. The interval between these cavities is 0.025 mm for case 1 I and II, and 0.01 mm for case 1 III and IV. In addition, for case 1 I and III, the cavities distribute in the fiber center, and for case 1 II and IV, the location of these cavities is  $5 \mu\text{m}$  away from the fiber center. In case 1 V, two cavities are in the radial direction. All details for case 1 are illustrated in Figure 8. Case 2 simulates the fiber specimens with different sizes of interior cavities

and the distribution of these cavities is the same as case 1 I. Figure 9 gives the fiber specimen mesh with different size of cavities.

The simulation results are listed in Table 3. The fiber with interior cavities along its central axis has higher breaking load and breaking extension than the fibers with cavities located away from the central axis (see Figure 8 I, III and Figure 8 II and IV). This suggests that the stress concentration develops more easily around cavities away from the fiber center. Considering the density of the distribution of the cavities (see Figure 8 I and III or Figure 8 II and IV), we have found that the higher the density, the lower the breaking load and breaking extension. As three cavities distribute closely, the tensile stress in this region concentrates severely, the fiber is therefore weaker and the breaking load and breaking extension decrease. The results are also consistent with the results obtained by Karbhari and Wilkins [32]. But the



A: the coarsest fibre segment  
 B: distance of 0.01 mm from C  
 C: the thinnest fibre segment

**Figure 10.** The different locations of (a) transverse crack and (b) longitudinal crack.

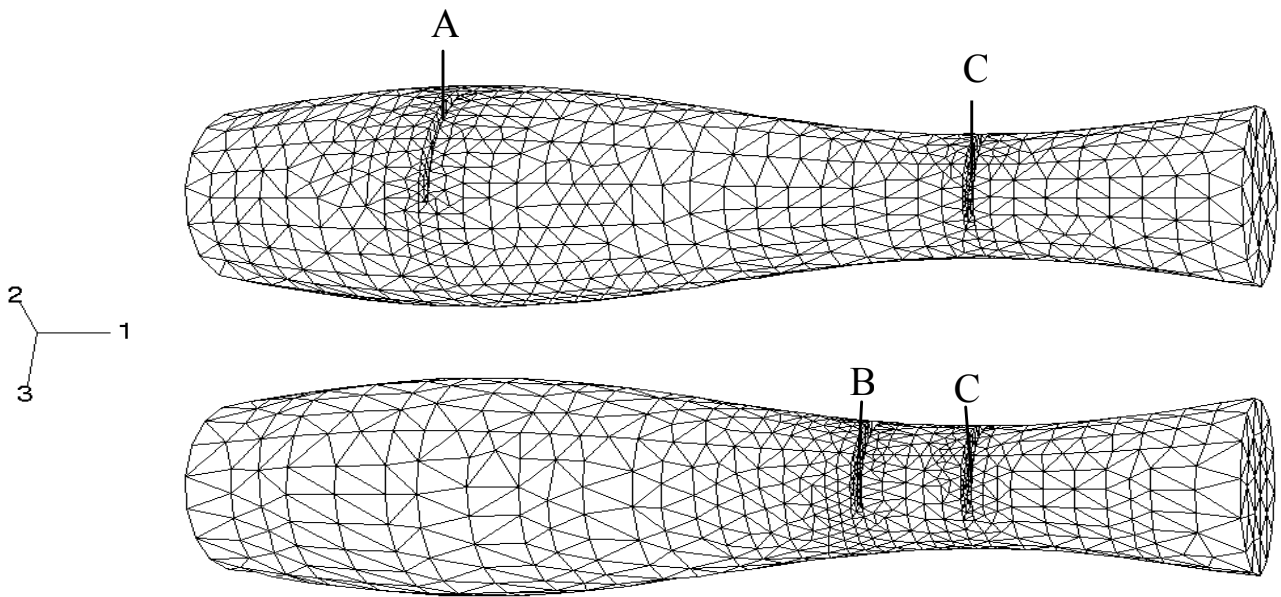


**Figure 11.** Graphical representations of two transverse cracks at different locations.

values vary slightly by either changing the location of the cavities or the density. However, when two

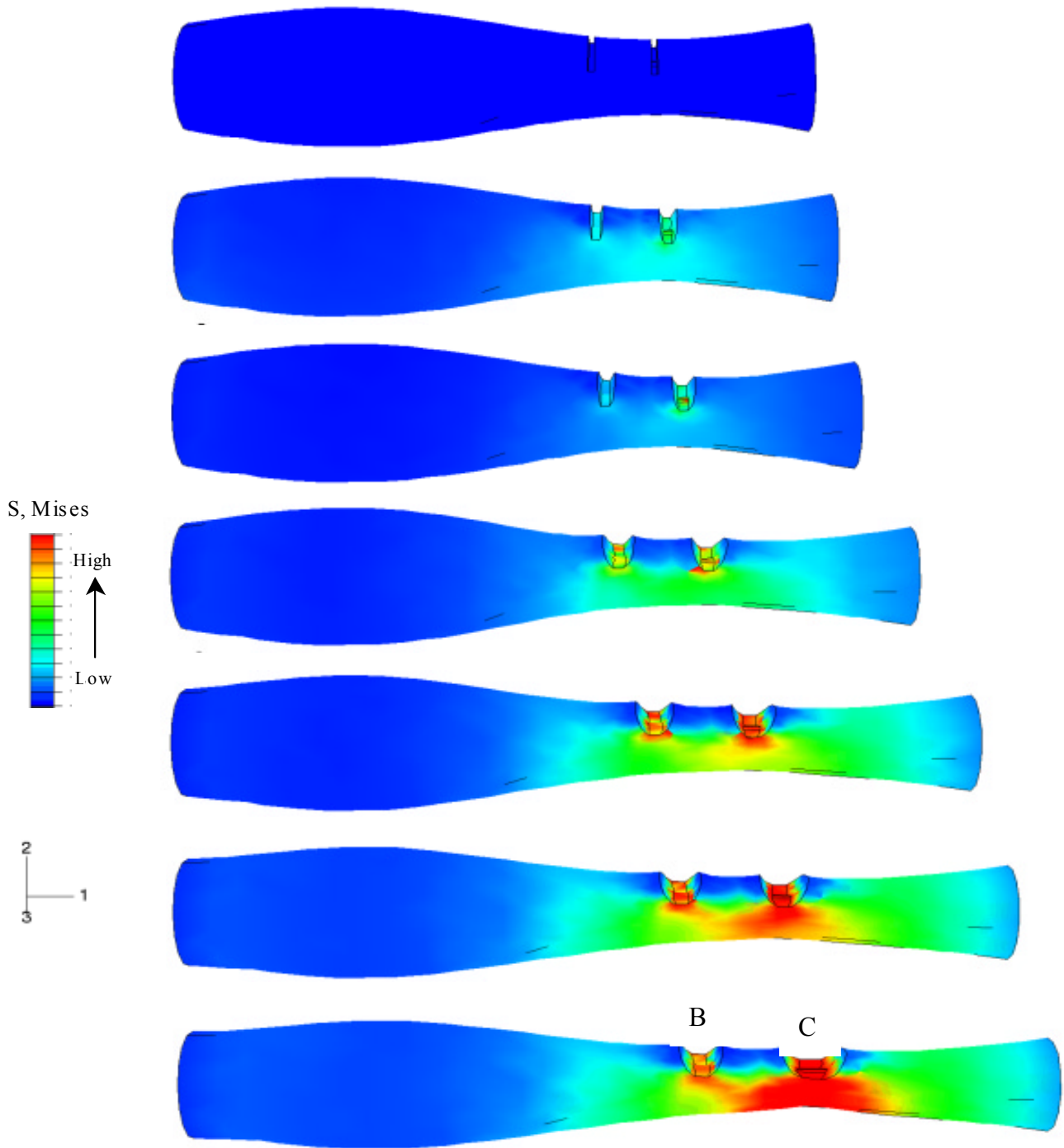


**Figure 12.** The contours of equivalent stress of a fiber with two transverse cracks located at B and C segments during successive extensions.

cavities are in the radial direction and another cavity is located along the fiber length (Figure 8

V), as two cavities in the radial direction cause a further reduction in fiber cross-sectional area, the

**TABLE 4. Simulation Condition and Data for Fiber Specimen with Different Location and Size of Surface Crack.**

Simulation cases		Crack type	Crack location	Crack size (Unit: $\mu\text{m}$ )	Simulation results	
					Breaking load (g)	Breaking extension (%)
Case 1		No crack	-	0	2.48	42.2
Case 2	I	Transverse crack	A	15 x 1 x 4	2.48	42.2
	II		B		2.29	40.5
	III		C		1.97	34.3
Case 3	I	Longitudinal crack	A		2.48	42.2
	II		B		2.45	41.6
	III		C		2.42	41.0
Case 4	I	Transverse crack	A	15 x 1 x 8	2.48	42.2
	II		B		1.82	32.0
	III		A	15 x 2 x 4	2.48	42.2
	IV		B		2.26	40.1
Case 5	I	Two transverse cracks	A + C	15 x 1 x 4	2.01	35.1
	II		B + C		2.03	35.9

fiber is weaker than other cases. Therefore, the breaking load and breaking extension of the fiber specimen decreases significantly.

When the diameter of interior cavities of the fiber specimen varies (see Figure 9), the tensile behavior of the fiber will be affected. The breaking load and breaking extension decrease markedly with the increase in the diameter of interior cavities (see Table 3 case 1 I and case 2). The results also show that the size of the cavity plays a more prominent role in determining fiber tensile properties than the cavity distribution, which is in agreement with the experimental results obtained by Taylor et al. [30].

### 3.2 Effect of Fiber Structural and Dimensional Variation on Fiber Tensile Behavior

The dimensional variation of fiber specimen is considered here, which follows the sine wave pattern and has a 30% level of diameter variation in the simulations, together with flaws distributed in it. The length and average diameter of fiber specimen are also 0.1 mm and 20  $\mu\text{m}$ , respectively.

#### 3.2.1 Effect of Type, Location and Size of Surface Crack on Fiber Tensile Behavior

We simulate five cases here. Case 1 represents the fiber specimen with a 30 % level of diameter

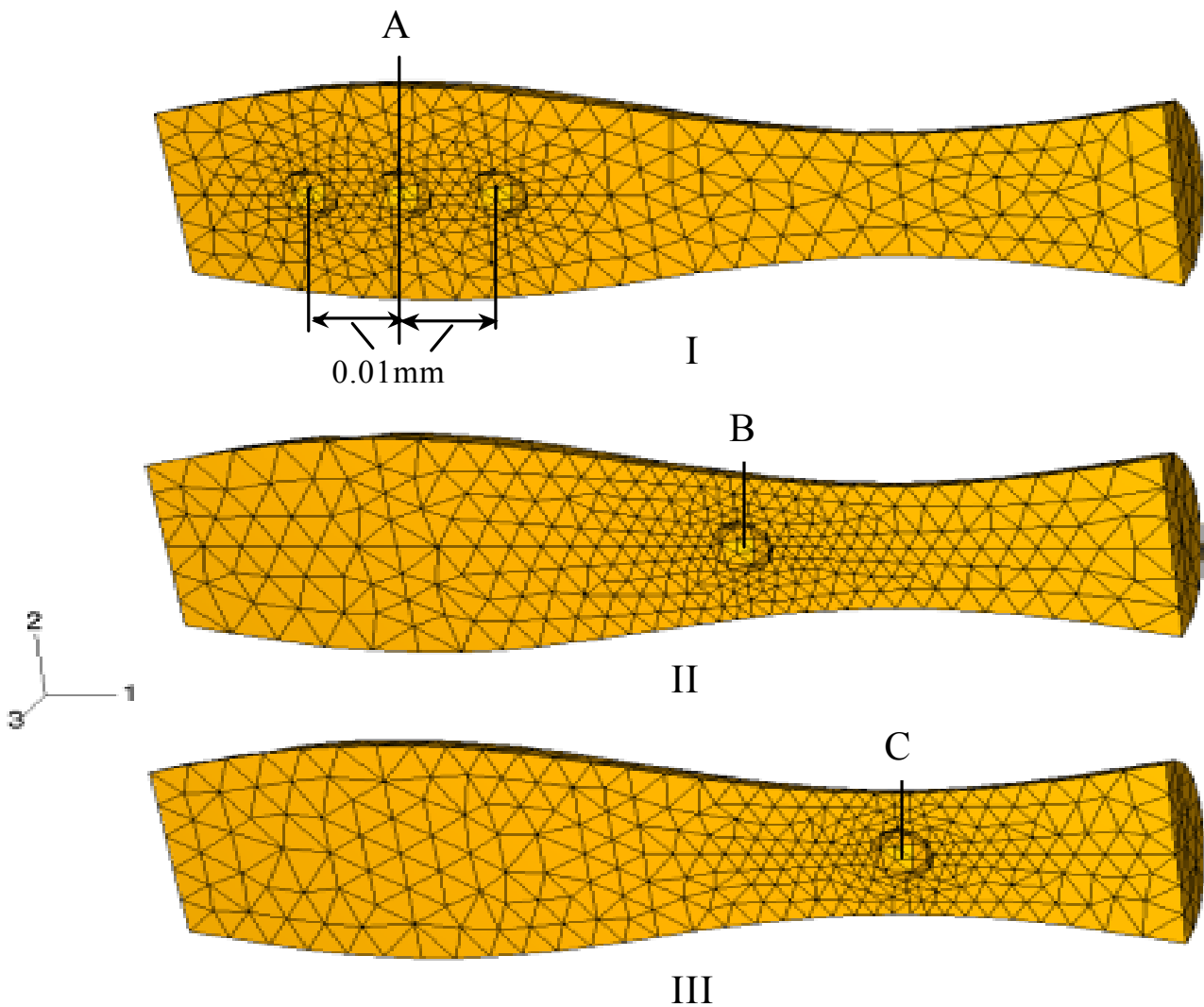


**Figure 13.** Finite element mesh of different location of interior cavity(s).

variation and without any surface and interior flaws. Case 2 and Case 3 simulate the fiber specimen with a surface transverse and longitudinal cracks and the crack is located in three different positions A, B and C along the fiber, respectively, as shown in Figure 10. Case 4 is the same as Case 2, but the size of the crack is changed (see Table 4). Case 5 simulates the fiber specimen with two transverse cracks, but with different locations along the fiber, as illustrated in Figure 11. Table 4 lists the breaking load and breaking extension of the simulated fiber specimen for all

different cases described above.

For Case 2 I, Case 3 I and Case 4 I, III, the fiber all has one crack, which is located at the coarsest segment A of fiber, but the crack type and size are different. When the fiber is stretched, the values of the breaking load and breaking extension are all the same as the fiber only with dimensional variation (case 1). As the crack in all of these cases does not lead to the reduction in the minimum cross-sectional area of fiber and the fiber will break at the thinnest segment C. Consequently, the breaking load and breaking extension are not

**Table 5: Simulation Condition and Data for Fiber Specimens with Interior Cavities at Different Locations.**

Simulation Cases		Cavity(s) location	Simulation results	
			Breaking load (g)	Breaking extension (%)
Case 1		No	2.48	42.2
Case 2	I	A (three cavities)	2.48	42.2
	II	B	2.46	41.6
	III	C	2.19	37.7

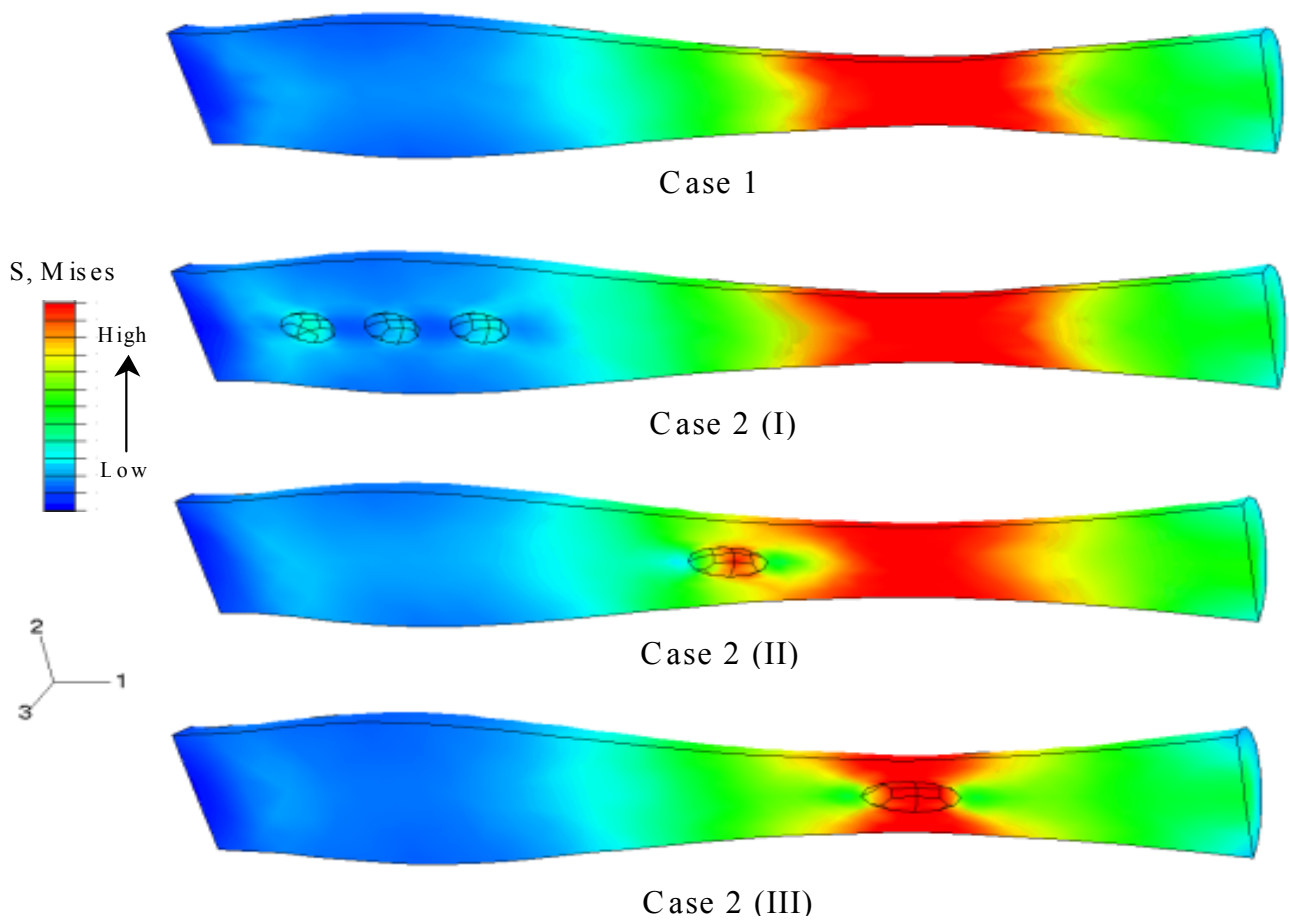


**Figure 14.** The contours of distribution of equivalent stress of a fiber for different cases at the last deformation step.

changeable for these cases.

When the transverse crack or longitudinal crack

is located at the thinnest segment C of fiber, undoubtedly, the minimum cross-sectional area of



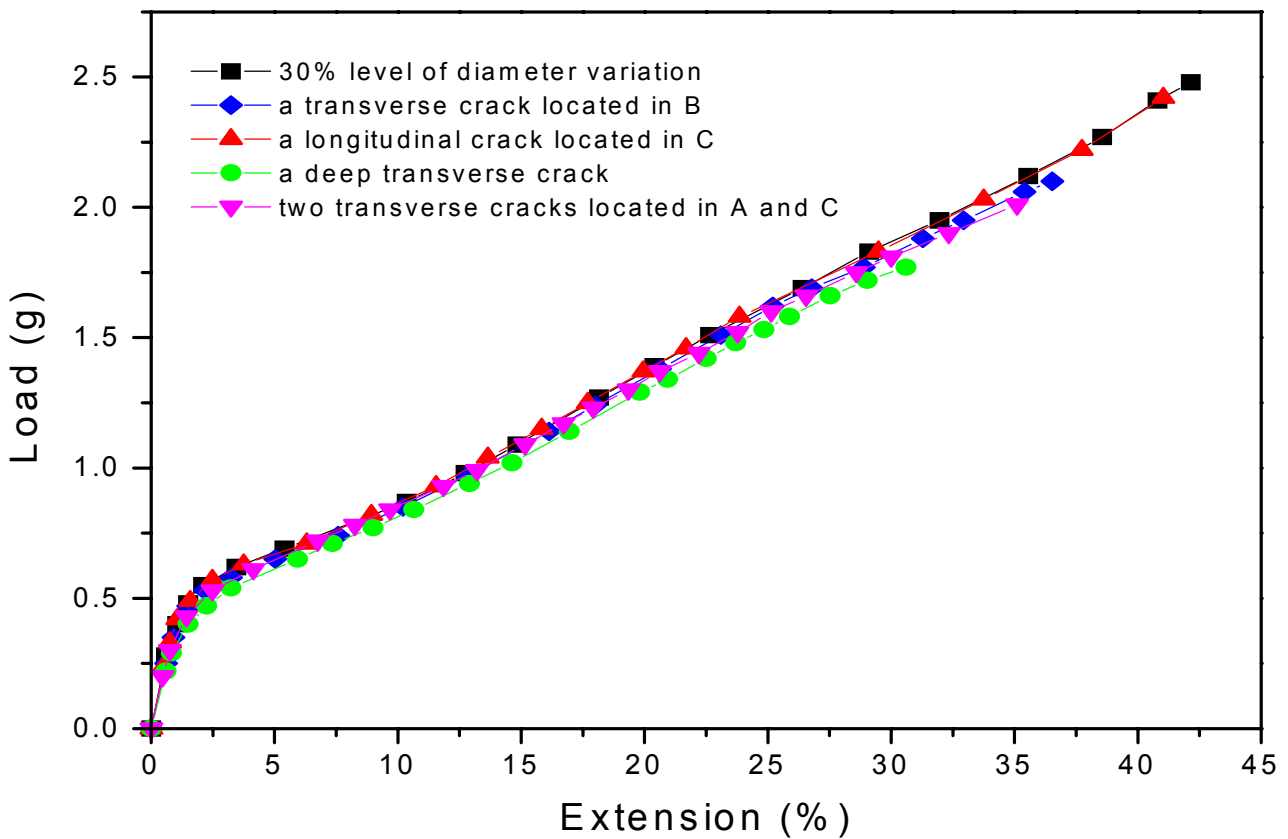


Figure 15. Load-extension curves of fibers with dimensional variation and different flaws.

fiber has a marked decrease. The breaking load and breaking extension of the fiber are bound to decrease (see case 2 III and case 3 III) and for the other case, the transverse crack or longitudinal crack is located at neither the coarsest nor the thinnest segment of the fiber, which is at a distance of 0.01 mm (B) from the thinnest segment (C) (Figure 10). In this position, the crack with a depth of 4  $\mu\text{m}$  results in a reduction of the fiber cross-sectional area, but this cross-sectional area is still larger than that of the thinnest segment C with the same crack and lower than the thinnest segment without the crack. Therefore, the values of fiber breaking load and breaking extension are between that of two cases. However, whether the crack is located at (B) or (C), the reduction in breaking load and breaking extension of the fiber with a transverse crack is more than the fiber with a

longitudinal crack (case 2 II and Case 3 II, case 2 III and Case 3 III). This result is the same as the previous result discussed in Section 3.1.1 and also can be explained using the stress distribution and the size of cross-sectional area where the crack is located.

When the depth (case 4 I) or width (case 4 II) of the transverse crack at the B segment increases, the breaking load and breaking extension of the fiber decrease. And the fiber with a deep crack is also weaker than the fiber with a wide crack, which is also agreement with the previously results in Section 3.1.1.

Two transverse cracks are located at two different segments of the fiber, as shown in Figure 11. The simulation results are listed in Table 4, case 5. It is very interesting to compare the simulation results for Case 5 and Case 2 III. When there is a crack in

the fiber section with the minimum cross-sectional area, adding an identical crack to another section of the fiber actually improves the fiber breaking load and breaking extension slightly. This suggests that an increased number of the crack is sharing the tensile stress when the fiber is stretched, which contributes to the increased breaking load and breaking extension. The sharing the tensile stress can be clearly observed in Figure 12, in which the tensile stress not only concentrates on the thinnest segment C, but also on the segment B at increasing extensions. Ultimately, the fracture of the fiber still occurred at the weakest - thinnest segment.

### 3.2.2 Effect of Location of Interior Cavities on Fiber Tensile Behavior

As shown in Figure 13, the cavities simulated here are located at A, B and C, respectively. In case 2 I, three cavities are distributed in the coarse segment of fiber specimen and the middle cavity is located at the coarsest segment A, Cases 2 II and III have one cavity only, located in B and C, respectively. The cavities distribute in the fiber center in all these cases.

Table 5 lists the results from the FE model. The results indicate that the breaking load and breaking extension decrease when the cavities are located in segments B and C of the fiber, respectively, and the values decrease slightly for the former and markedly for the latter. But the values are the same as the fiber without any cavities even though three cavities occur at the coarsest segment A (see Case 1 and Case 2 I). Figure 14 plots the contours of distribution of equivalent stress of a fiber for different cases at the last deformation step, in which the maximum stress is always distributed in the weakest segment of fiber specimen. This result is also consistent with the results obtained from the study of the surface crack in Section 3.2.1. This proves that the flaw location is more important than the flaw type in determining fiber tensile properties.

Investigation of combined dimensional and structural variations of fibers shows that for fiber specimen with crack or cavity, their shapes of load-extension curves are all the same as that the fibers with a 30 % level of diameter variation and without any flaws. But the breaking point varies with fiber flaw type, size and location. The load-extension curves for some cases are shown in

Figure 15.

To further compare Figure 7 with Figure 15, an important result is that the effect of dimensional variation of fiber on fiber tensile properties is larger than that of structural irregularity. Dimensional variation of fiber leads to a marked reduction in breaking load and breaking extension and also changes in the shape of load-extension curves. The structural irregularity of fiber only affects the values of breaking load and breaking extension.

## 4. CONCLUSIONS

A three-dimensional finite-element model has been utilized to investigate the tensile behavior of fibers with simulated structural irregularities and combined dimensional and structural variations, respectively. The following conclusions can be drawn from this study:

- The model prediction agrees with previous research in that a fiber always breaks at its weakest point. Dimensionally uniform fibers would break at the position of fiber flaws or defects. For fibers with both dimensional and structural irregularities, their combined effect will determine where the weakest point is, and hence where the fiber breaks.
- The fiber with a transverse crack leads to more reduction in the breaking load and breaking extension than the fiber with a similar longitudinal crack, and with increasing depth and width of the crack, the breaking load and breaking extension decrease. This can be attributed to the reduction in fiber cross-sectional area.
- The size of the interior cavity plays a more prominent role in determining the breaking load and breaking extension of the fiber than the distribution of the cavity. The larger the cavity, the lower the breaking load and breaking extension.
- For a fiber with dimensional variation, the flaw location influences the breaking load and breaking extension of the fiber more than the flaw type. The values of the breaking load and breaking extension will decrease when the structural flaw leads to a net reduction in the minimum cross-sectional area of the irregular fiber.
- Fiber geometrical or dimensional variations have a marked influence on the tensile properties of the fiber. It affects not only the values of the breaking

load and extension, but also the shape of the load-extension curves. However, the fiber structural irregularities simulated in this study appear to have little effect on the shape of the load-extension curves.

## 5. REFERENCES

1. Banky, E. C. and Slen, S. B., "Note on the Effect of Nonuniformity of the Cross-sectional Area Upon the Tensile Behavior of Wool fiber", *Text. Res. J.*, 25, (1955), T358-361.
2. Banky, E. C. and Slen, S. B., "Dimensional Changes and Related Phenomena in Wool Fibers Under Stress", *Text. Res. J.*, 26, (1956), 204-210.
3. Kenny, P. and Chaikin, M., "Stress-Strain-Time Relationships of Non-uniform Textile Materials", *J. Text. Inst.*, 50, (1959), T18-T40.
4. Collins, J. D. and Chaikin, M., "Dimensional Relations in Unstrained and Strained Wool Fibers", *J. Text. Inst.*, 57, (1966), T45-T54.
5. Shah, S. M. A. and Whiteley, K. J., "Variations in the Stress-Strain Properties of Wool Fibers", *J. Text. Inst.*, 57, (1966), T286-T293.
6. Wang, X., "Predicting the Strength Variation of Wool from Its Diameter Variation", *Text. Res. J.*, 70(3), (2000), 191-194.
7. Zhang, Y. and Wang, X., "The Effect of Along-Fiber Diameter Variation on Fiber Tensile Behavior", *Wool Tech. Sheep Breed.*, 48(4), (2000), 303-312.
8. Zhang, Y., "The Tensile Behavior of Non-Uniform Fibers and Fibrous Composites", Ph.D Thesis, School of Eng. and Tech. Deakin University, (2001).
9. Collins, J. D., "Fiber Non-Uniformity and Its Effect on Fiber Rheological Behavior", Ph.D thesis, University of New South Wales, (1964).
10. Collins, J. D. and Chaikin, M., "The Longitudinal and Torsional Behavior of Non-Uniform Wool Fibers", *Third International Wool Textile Research Conference*, (Section 1), Paris, France, (1965), 571-580.
11. Collins, J. D. and Chaikin, M., "The Longitudinal Rheological Behavior of Non-Uniform Fibers", *Text. Res. J.*, 35(8), (1965), 679-693.
12. Collins, J. D. and Chaikin, M., "Some Aspects of Wool Fiber Non-Uniformity", *Third International Wool Textile Research Conference* (Section 1), Paris, France, (1965), 581-592.
13. Collins, J. D. and Chaikin, M., "The Stress-Strain Behavior of Dimensionally and Structurally Non-Uniform Wool Fibers in Water", *Text. Res. J.*, 35(9), (1965), 777-787.
14. Collins, J. D. and Chaikin, M., "Structural and Non-Structural Effects in the Observed Stress-Strain Curve for Wet Wool Fibers", *J. Text. Inst.*, 59, (1968), 379-401.
15. Collins, J. D. and Chaikin, M., "A Theoretical and Experimental Analysis of the General Wool Fiber Stress-Strain Behavior with Particular Reference to Structural and Dimensional Nonuniformities", *Text. Res. J.*, 39, (1969), 121-139.
16. Feughelman, M., "A Two-Phase Structure for Keratin Fibers", *Text. Res. J.*, 29, (1959), 223-228.
17. Feughelman, M., "Mechanical Properties and Structure of Alpha-Keratin Fibers, Wool, human Hair and related Fibers", University of New South Wales, Sydney, (1997), 28-58.
18. Mason, P., "The Fracture of Wool Fibers Part I: The Viscoelastic Nature of the Fracture Properties", *Text. Res. J.*, 34, (1964), 747-754.
19. Andrews, M. W., "The Fracture Mechanism of Wool Fibers Under Tension", *Text. Res. J.*, 34, (1964), 831-835.
20. Makinson, K. R., "Fracture in Wool Fibers (Letters to the Editor)", *J. Text. Inst.*, 60, (1969), 151-153.
21. Gharehaghaji, A. A. and Johnson, N. A. G., "Wool-Fiber Microdamage Caused by Opening Processes Part I: Sliver Opening", *J. Text. Inst.*, 84, (1993), 336-347.
22. Gharehaghaji, A. A. and Johnson, N. A. G., "Wool Fiber Microdamage Caused by Opening Processes Part II: A Study of the Contact Between Opening Elements and Wool Fiber in Controlled Extension", *J. Text. Inst.*, 86, (1995), 402-414.
23. Gharehaghaji, A. A., "Wool Fiber Microdamage Due to Contact Stresses in Opening Processes", ph.D thesis, University of New South Wales, (1994).
24. Wang, X., "Damage to Wool Fibers Opened by Vibrating Strings", *J. Text. Inst.*, 86(3), (1995), 492-494.
25. Wang, L. and Wang, X., "A Study of Wool's Tensile Strength in Early Stage Processing", *Text. Res. J.*, 70(2), (2000), 98-102.
26. Wang, L. and Wang, X., "A Study of Fiber Strength Loss in Simulated Fiber Opening Processes", The 6th Asian Textile Conference, Hong Kong, (2001).
27. Dalmaz, A., et al., "Damage Propagation in Carbin/Silicon Carbide Composites During Tensile Tests Under the SEM", *J. Mater. Sci.*, 31, (1996), 4213-4219.
28. Zinck, P., et al., "Mechanical Characterisation of Glass Fibers as an Indirect Analysis of the Effect of Surface Treatment", *J. Mater. Sci.*, 34, (1999), 2121-2133.
29. Sawyer, L. C., et al., "Strength, Structure, and Fracture Properties of Ceramic Fibers Produced from Polymeric Precursors: I, Base-Line Studies", *J. Am. Ceram. Soc.*, 70 (11), (1987), 798-810.
30. Taylor, S. T., et al., "Characterization of Nicalon Fibers with Caring Diameters Part I Strength and Fracture Studies", *J. Mater. Sci.*, 33, (1998), 1465-1473.
31. Jones, J. B., Barr, J. B. and Smith, R., "Analysis of Flaws in High-Strength Carbon Fibers from Mesophase Pitch", *J. Mater. Sci.*, 15, (1980), 2455-2465.
32. Karbhari, V. M. and Wilkins, D. J., "Significance of Longitudinal and Transversal Size Effects on the Statistics of Fiber Strength", *Philosophical Magazine A*, 64 (6), (1991), 1331-1344.
33. Knoff, W. F., "Combined Weakest Link and Random Defect Model for Describing Strength Variability in Fibers", *J. Mater. Sci.*, 28, (1993), 931-941.
34. Wisnom, M. R., "Modeling the Effect of Cracks on Interlaminar Shear Strength", *Composites Part A*, 27A, (1996), 17-24.
35. Tong, J., et al., "On Matrix Crack Growth in Quasi-

- Isotropic Laminates - II. Finite Element Analysis", *Composites Science and Technology*, 57, (1997), 1537-1545.
36. Firmature, R. and Rahman, S., "Elastic-Plastic Analysis of Off-Centre Cracks in Cylindrical Structures", *Engineering Fracture Mechanics*, 66, (2000), 15-39.
37. Zhang, W. and Subhash, G., "An Elastic-Plastic-Cracking Model for Finite Element Analysis of Indentation Cracking in Brittle Materials", *International Journal of Solids and Structures*, 38, (2001), 5893-5913
38. ABAQUS, ABAQUS/CAE User's Manual, Version 6.1. Hibbit, Karlsson and Sorensen, Inc., (2000).